

ICONN 2015 [4th -6th Feb 2015]
International Conference on Nanoscience and Nanotechnology-2015
SRM University, Chennai, India

Effect of mechanical milling on the cation distribution and Infrared spectral study of nano-structured $\text{CuAl}_x\text{Cr}_x\text{Fe}_{2-2x}\text{O}_4$ system

D. K. Mehta^{1*}, M.C.Chhantbar² and H. H. Joshi³

¹Government Science College, Ahmedabad, Guajrat, India.

²Shakersinh Vaghela Bapu Institute of Technology, PO-Vasan,
Dist-Gandhinagar, Gujarat, India.

³Department of Physics, Saurashtra University, Rajkot, Gujarat, India.

Abstract: $\text{CuAl}_x\text{Cr}_x\text{Fe}_{2-2x}\text{O}_4$ with $x=0.2$ and 0.6 ferrite nano-particles having dimensions varying between 14-29 nm, have been prepared by using solid-state reaction technique followed by high- energy ball milling for different time durations. EDAX and SEM characterizations have been carried out for the un-milled samples to ensure the stoichiometry and to reveal surface morphology of the samples, respectively. The structural and microstructural evolution of the nano-phase has been studied by x-ray powder diffraction technique. X-ray diffraction study of un-milled and milled samples explicates cation redistribution and structural transformation from cubic to tetragonal symmetry after 24hr of ball-milling. On the basis of cation distribution, some physical parameters like ionic radii (r_A , r_B), bond length (A-O, B-O), Oxygen parameter (u) and site radii have been calculated and it is observed that the milling process has marked influence on cation redistribution. Infrared absorption spectroscopy has been used to study the occurrence of various absorption bands in the spectra and these have been analyzed on the basis of cation distribution of the spinel lattice. The change in the band positions with increased milling time is observed because of the metal-ion oxygen distances and reduction in particle size. The elastic constants of the samples have been calculated by using infrared spectral data and x-ray diffraction pattern analysis at 300 K. The force constants for tetrahedral and octahedral sites determined by infrared spectral analysis have been used to calculate elastic constants and they are found to vary in accordance with variation of lattice constant and milling times.

Keywords: mechanical milling, cation distribution, Infrared spectral, nano-structure, $\text{CuAl}_x\text{Cr}_x\text{Fe}_{2-2x}\text{O}_4$ system.

Introduction

In recent years, nano-crystalline spinel ferrites have been investigated intensively because the miniaturization of functional electronic devices demands the placement of nanometer scale components into well-defined structures. As the size reduces into the nanometer range, the materials exhibit interesting electrical and magnetic properties compared to conventional coarse grained counterparts¹. The technique of high energy ball milling has been the subject of great interest for preparation of nanostructured material because of its

simplicity and relatively inexpensive equipment needed and the applicability essentially to all classes of materials.

The Cu-Fe-O system is of long standing interest in solid state physics, mineralogy and metallurgy. Due to a relatively small energy difference between Cu^{2+} ions in the A and B sites², cation redistribution is possible and strongly dependent upon the nano-range particle size along with various milling times. Moreover, the substitution of nonmagnetic ions like Al^{3+} and Cr^{3+} in simple and mixed ferrite changes the structural and magnetic properties. Infrared spectroscopy is one of the most powerful analytical techniques, which offers the possibility of chemical identification. Infrared spectral evolution of mechanically milled Ni-Zn ferrite has been reported earlier³. The effect of thermal history and irradiation on the structural properties of the bulk samples of spinel system $\text{CuAl}_x\text{Cr}_x\text{Fe}_{2-2x}\text{O}_4$ has been studied⁴. However, cation redistribution and elastic parameters influenced by ball milling in nanostructured Copper ferrite have not been investigated in detail. The purpose of the present work is to study structural changes along with cation redistribution and to characterize the prepared materials in terms of physical parameters by x-ray diffraction pattern analysis and infrared spectroscopy.

Experimental Details

Two compositions ($x=0.2$ and 0.6) of spinel ferrite system $\text{CuAl}_x\text{Cr}_x\text{Fe}_{2-2x}\text{O}_4$ prepared in bulk quantity (about 20 g) by standard double sintering ceramic technique were milled for 12h and 24h using high energy planetary ball mill (Fritsch, Pulverisette 6) with tungsten carbide vials and balls. The stoichiometry of the powder sample was checked by Energy Dispersive Analysis of X-rays (EDAX) and SEM (scanning electron micrographs) characterizations were recorded for ensuring the surface morphology. The samples were characterized by X-ray diffractometry using $\text{Cu K}\alpha$ radiation at 300 K. The infrared spectra in the wave number range $400\text{-}4000\text{ cm}^{-1}$ were recorded at 300 K using Perkin-Elmer made IR spectrometer.

Results and Discussion

Energy Dispersive Analysis of X-rays (EDAX) and Scanning Electron Micrographs (SEM):

A representative energy dispersive analysis of X-rays (EDAX) Pattern for composition $x=0.2$ and $x=0.6$ are shown in figure 1. No trace of any impurity was found indicating the purity of the samples. The result suggests that the precursors have fully undergone the chemical reaction to form the expected ferrite compositions and all the peaks are well assigned in accordance with the standard positions, which confirms the stoichiometry of each sample.

The Scanning Electron Micrograph (SEM) for un-milled samples of compositions $x=0.2$ and 0.6 of $\text{CuAl}_x\text{Cr}_x\text{Fe}_{2-2x}\text{O}_4$ ferrite system are shown in figure 2. It is seen that grain morphology, grain size and uniformity are highly influenced by Al^{+3} and Cr^{+3} substitutions. The reduction in grain size with increase the substitution of Al^{+3} and Cr^{+3} may explain on the basis of the cation distribution in the samples.

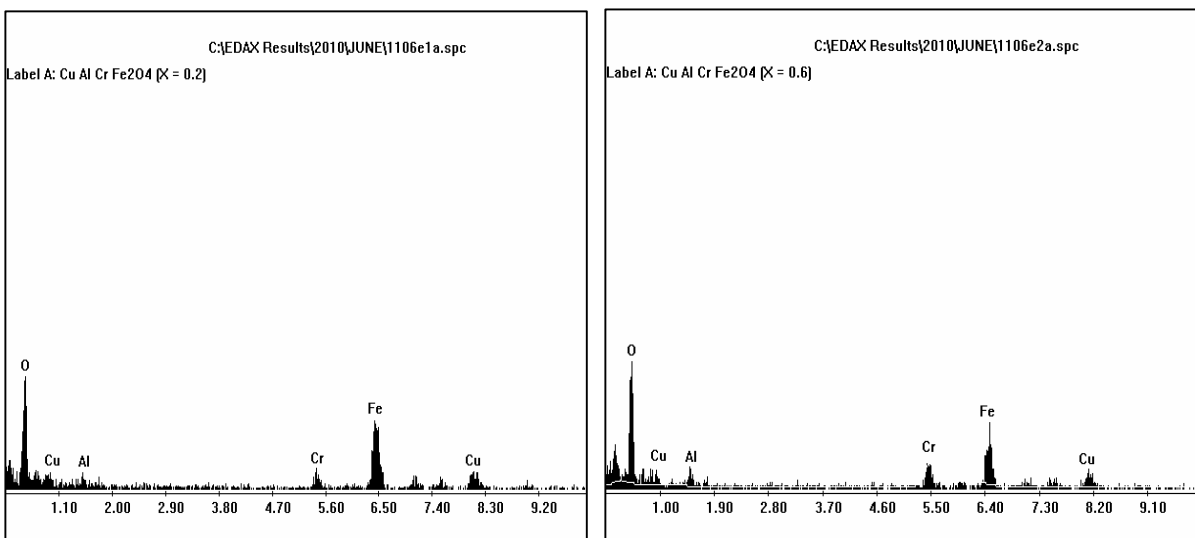


Figure 1. EDAX patterns for $x=0.2$ and $x=0.6$ compositions of $\text{Cu Al}_x\text{Cr}_x\text{Fe}_{2-2x}\text{O}_4$ system.

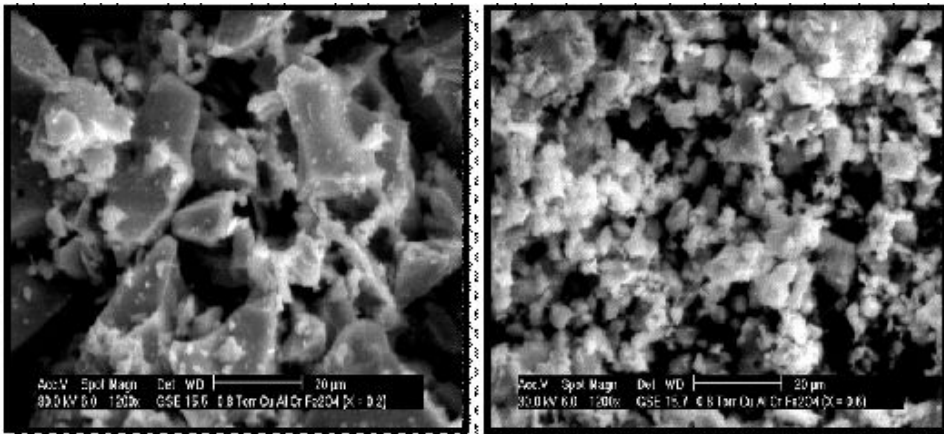


Figure 2. SEM images for unmilled samples of $x=0.2$ and 0.6 for $\text{CuAl}_x\text{Cr}_x\text{Fe}_{2-2x}\text{O}_4$ system.

X-ray powder diffraction data and cation distribution:

The room temperature x-ray diffraction patterns for un-milled and milled samples for various milling times for $x=0.2$ and 0.6 compositions are shown in figure 3. The un-milled and ball milled samples with milling time 12h for $x=0.2$ and $x=0.6$ are found to be single cubic phase and can be indexed with the face centered cubic (fcc) spinel structure of space group O_h^7 (Fd3m). The ball milled samples for $x=0.2$ and $x=0.6$ with 24h milling time show the remarkable change from cubic to tetragonal distortion due to the presence of Cu^{2+} Jahn-Teller ion at the B-site along with cation redistribution. The values of Lattice constant (a), Bulk density (ρ), x-ray density (ρ_x) and grain size D for $\text{CuAl}_x\text{Cr}_x\text{Fe}_{2-2x}\text{O}_4$ ferrite System are shown in table 1.

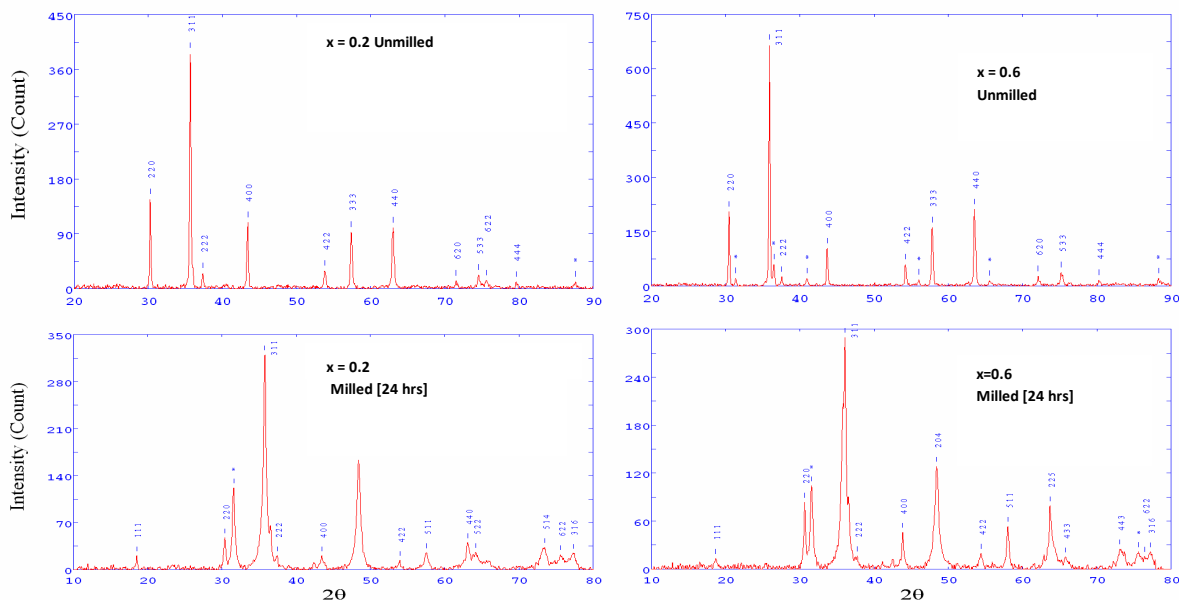


Figure 3. X-ray diffraction patterns of the system $\text{CuAl}_x\text{Cr}_x\text{Fe}_{2-2x}\text{O}_4$ ($x=0.2, 0.6$).

From the Debye Scherrer formula⁵, it is found that the average grain size decreases from 24nm to 19nm for 12h and 24 h milled samples for $x=0.2$ composition and 29 nm to 14 nm for 12h and 24h milled samples for $x=0.6$ composition. The size of the grain decreases as the milling time increases because the kinetic energy generated by the series of collisions among balls is transferred to the system⁶. The x-ray density (ρ_x) of the samples is determined using relation given by Smith and Wijn⁷. Due to the pores in the samples, it is observed that x-ray density ρ_x of each sample is greater than the corresponding bulk density ρ . The values of bulk density is observed to decrease with increase of the substitution Al^{3+} and Cr^{3+} from $x=0.2$ to $x=0.6$. Moreover, there is decrease in bulk density with increased milling time from 12h to 24h. The decrease in bulk density for $x = 0.2$ and 0.6 may be the number of pores are increased due to the micro-structural changes brought about by the sintering condition. The same theory may apply for the decrease in bulk density with increased milling time.

Table 1. Lattice constant (a), Bulk density (ρ), X-ray density (ρ_x), Grain size (D) Ionic radii (r_A , r_B), bond lengths (A-O, B-O), oxygen positional parameter (u) and site radii (R_A , R_B) for $\text{CuAl}_x\text{Cr}_x\text{Fe}_{2-2x}\text{O}_4$ ferrite system.

Structural Parameters	x = 0.2			x = 0.6		
	Un-milled	Milled		Un-milled	Milled	
		12 hrs	24hrs		12 hrs	24hrs
Lattice constant $a(\text{\AA}) \pm 0.002\text{\AA}$	8.338	8.3451	a=b=8.321 c=8.394 c/a=1.008	8.281	8.257	a=b=8.228 c=8.420 c/a=1.023
Bulk density(ρ) (kg/m^3) $\times 10^3$	5.025	4.903	4.937	4.235	3.770	3.764
X-ray density(ρ_x) (kg/m^3) $\times 10^3$	5.332	5.320	5.319	5.139	5.183	5.118
Grain size D (nm)	---	24	19		29	14
r_A (\AA)	0.622	0.643	0.712	0.664	0.688	0.630
r_B (\AA)	0.675	0.664	0.630	0.626	0.614	0.643
A – O (r_A+R_O)	1.942	1.963	2.032	1.984	2.008	1.950
B – O (r_B+R_O)	1.995	1.984	1.950	1.946	1.934	1.963
u^{3m} (\AA)	0.2613	0.2654	0.2657	0.2630	0.2657	0.2642
R_A (\AA)	1.9684	2.0293	2.0277	1.9704	2.0102	1.9837
R_B (\AA)	1.9947	1.9662	1.9583	1.9597	1.9414	1.9472

Cation arrangement is not unique in spinel ferrites. The distribution of the cations in the tetrahedral (A) and octahedral (B) interstitial sites of the spinel lattice was determined through x-ray diffraction intensity analysis using the computer program based on the Buerger's formula⁸. According to Ohnishi and Teranishi⁹, the intensity ratios of planes I(2 2 0)/I(4 4 0), I(4 0 0)/I(4 2 2) and I(2 2 0)/I(4 0 0) are considered to be sensitive to the any change in cation distribution. During the analysis it was assumed that the Cu^{2+} ions maintains its 90% degree of inversion as in CuFe_2O_4 throughout the system and the occupancy of Cr^{3+} was fixed for octahedral site due to its well-known B-site preference according to the ionic configuration based on site preference energy values proposed by Miller¹⁰ for individual cation. The occupancies of the Al^{3+} and Fe^{3+} ions were varied and the results of the calculated and observed XRD intensities were compared repeatedly. The comparisons of x-ray diffraction intensity ratios for various possible cation distributions for unmilled and milled compositions are shown in table 2.

Table 2. Results of XRD intensity analysis and Cation distributions for samples of $\text{CuAl}_x\text{Cr}_x\text{Fe}_{2-2x}\text{O}_4$ system.

x	sample	Cation Distribution		I220/I440		I400/I422		I220/I400	
		A-site	B-site	Cal.	Obs.	Cal.	Obs.	Cal.	Obs.
0.2	Unmilled	($\text{Cu}_{0.1}\text{Al}_{0.2}\text{Fe}_{0.7}$)	($\text{Cu}_{0.9}\text{Cr}_{0.2}\text{Fe}_{0.9}$)	0.51	1.35	3.18	3.22	0.91	1.39
	12 h milled	($\text{Cu}_{0.2}\text{Al}_{0.1}\text{Fe}_{0.7}$)	($\text{Cu}_{0.8}\text{Al}_{0.1}\text{Cr}_{0.2}\text{Fe}_{0.9}$)	0.58	1.19	2.48	2.46	1.16	1.84
	24 h milled	($\text{Cu}_{0.9}\text{Fe}_{0.1}$)	($\text{Cu}_{0.1}\text{Al}_{0.2}\text{Cr}_{0.2}\text{Fe}_{1.5}$)	0.77	1.18	1.37	1.49	2.10	2.28
0.6	Unmilled	($\text{Cu}_{0.30}\text{Fe}_{0.7}$)	($\text{Cu}_{0.70}\text{Al}_{0.6}\text{Cr}_{0.6}\text{Fe}_{0.1}$)	0.76	0.97	1.49	1.77	1.96	1.96
	12 h milled	($\text{Cu}_{0.6}\text{Fe}_{0.4}$)	($\text{Cu}_{0.4}\text{Al}_{0.6}\text{Cr}_{0.6}\text{Fe}_{0.4}$)	0.83	1.26	1.24	1.99	2.34	2.32
	24 h milled	($\text{Cu}_{0.2}\text{Al}_{0.2}\text{Fe}_{0.6}$)	($\text{Cu}_{0.8}\text{Al}_{0.4}\text{Cr}_{0.6}\text{Fe}_{0.2}$)	0.59	1.05	2.41	2.34	1.19	1.81

In a variety of systems, it has been reported that high-temperature metastable phase could be formed during nonequilibrium dynamic milling process¹¹. Hence, due to nanometer sized grains, high local pressures and temperatures during collisions with balls and vial, the decomposition process of the final product might occur in the milling process, which may result in atomic disorder and abnormal as well as unexpected cation distribution. Thus, Milling is possible reason for nonlinear change in the structural and elastic parameters due to the rearrangement of cation distribution from bulk to milled samples for each composition.

In order to explain variation in lattice parameter for every composition and lattice expansion from 8.338 Å to 8.3451 Å for unmilled to 12h milled samples of $x=0.2$ composition, the value of the mean ionic radius per molecule of the A-and B-sites using the cation distribution have been calculated, using the relation¹². The bond lengths, B – O and A – O are average bond lengths and the oxygen positional parameter (u) for each composition can be calculated using the formulae available in the literature¹³.

The calculated values of, ionic radii (r_A, r_B), bond lengths (A-O, B-O), oxygen positional parameter (u) and site radii (R_A, R_B) are listed in table 1. It is observed that r_A increases and r_B decreases gradually for $x=0.2$ to $x=0.6$ composition and with increasing milling time for each composition. For 24h milled sample of $x=0.6$, reverse trend is observed, where r_A decreases and r_B increases slightly. This is due to the change in the distribution of cations among the A-and B-sites by milling. According to redistribution of cations, larger cation Cu^{2+} (0.73 Å) migrate to tetrahedral A-site and smaller cation Al^{3+} (0.535 Å) migrate to octahedral B-site with increased milling time. Therefore the change occurs in the mean ionic radius after milling. For 24h milled sample of $x=0.6$, the presence of smaller cation Al^{3+} at A-site causes the reverse trend. For both the composition, oxygen parameter u increases with increased milling time. The obtained data of bond lengths B-O and A-O and site radii R_A and R_B for unmilled and milled samples vary according to ionic radii r_B and r_A of octahedral (B) and tetrahedral (A) sites, respectively.

Infrared spectroscopy:

The room temperature (300K) infrared (IR) absorption spectra recorded in the wave number range 400-1000 cm^{-1} for all the samples are shown in figure 4. No IR active absorption bands were observed above 650 cm^{-1} . The bands in the 300 – 700 cm^{-1} region are assigned to the fundamental vibrations of the ions of the crystal lattice.

The high frequency band ν_1 , is in the range 580 - 610 cm^{-1} and the low frequency band, ν_2 , is in the range 470 – 515 cm^{-1} . The band positions for all the samples are given in table 3. The change in the band position is expected because of the difference in the metal ion-oxygen distances for the octahedral and tetrahedral complexes. It has been reported¹⁴ that Fe^{3+} - O^{2-} distance for the A-sites (1.86Å) is smaller than that of the B-sites (2.02Å). This can be interpreted by the stronger covalent bonding of Fe^{3+} ions at the A-sites than the B-sites. A keen inspection of the IR spectra reveals the fact that (a) the frequency band ν_1 and ν_2 are shifted to higher frequencies with an increasing Al-Cr concentration for both milled and unmilled samples. (b) low frequency band ν_2 for $x=0.2$ and 0.6 shifts towards higher frequency side for unmilled sample to 12 h milled sample, whereas, for 24h milled sample, it shifts slightly towards lower frequency side. (c) high frequency band ν_1 for $x=0.6$ shifts towards lower frequency side for unmilled sample to 12 h milled sample, whereas, for 24h milled sample, it shifts slightly towards higher frequency side. (d) No broadening of bands with milling time is observed. Earlier this type of broadening is reported¹⁵ in normal spinel ferrites.

The shifted position of the absorption band ν_1 for 12h milled samples to 24 h milled sample may be due to the decrease in particle size. This is a consequence of size effect³. For nanoparticles, small changes in the environment of a chemical group will lead to a small change in the characteristics vibration frequency for this group. Thus, as the particle size decreases the increase in centre frequency of absorption band is observed.

Table 3. Positions of IR main absorption bands (ν_1 and ν_2) for $\text{CuAl}_x\text{Cr}_x\text{Fe}_{2-2x}\text{O}_4$ ferrite system.

X	Samples	$\nu_1 \text{ cm}^{-1}$	$\nu_2 \text{ cm}^{-1}$
0.2	un-milled	580.2	470.7
	12h-milled	588.9	476.1
	24h-milled	594.3	474.1
0.6	un-milled	604.1	508.9
	12h-milled	599.2	514.4
	24h-milled	605.8	506

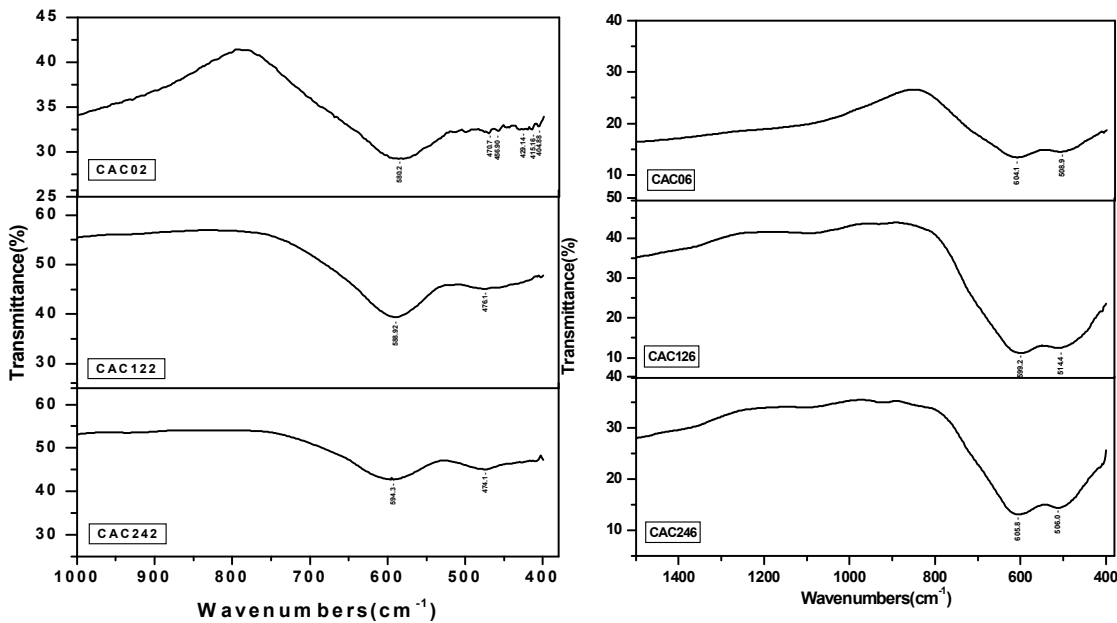


Figure 4. IR spectra of unmilled and milled samples for $x=0.2$ and 0.6 composition at RT for $\text{Cu Al}_x\text{Cr}_x\text{Fe}_{2-2x}\text{O}_4$ system.

The force constant, for tetrahedral site (k_t) and for octahedral site (k_o), average force constant (k) have been obtained from the IR data using the standard formulae suggested by Waldron¹⁶, which are listed in table 4. It is observed from the result that (a) the values of k_t and k increase and the value of k_o decreases with increase in Al-Cr content. (b) the average force constant k and k_t increase with increase in milling time and k_o decreases with increase in milling time for $x=0.2$ composition. (c) For $x=0.6$ composition, some abnormal change is observed. Here, the values of k_t and k increase with increasing milling time for unmilled to 12h milled sample, while for 24h milled sample k_t is found to decrease. The same trend is observed for k as a function of milling time, whereas k_o increases with increase of milling time. This change in k_t and k is attributed to same change in site radius R_A for $x=0.6$ composition which increases for unmilled to 12h milled sample and then slight decreases for 24h milled sample. This unexpected result can be attributed to the fact that under favorable conditions, oxygen can form stronger bonds with metal ions even at larger internuclear separations.

The calculated values of V_l , V_s , V_m , T_D , B , E , G and Poisson's ratio (ν) are listed in table 4 and all above parameters have been calculated using suggested formulae¹⁷. It is observed from the list that (a) there is increase for the values of V_l , V_s , V_m , T_D , B , E and G with increase Al-Cr content (b) there is increase for the values of V_l , V_s , V_m , T_D , B , E and G with increasing milling time (c) there is decrease for the values of V_l , V_s , V_m , T_D , B , E and G for 24h milled sample for $x=0.6$ composition (d) The Poisson's ratio remains constant 0.35 for all the samples. It is reported that grain size reduction induced by mechanical milling has small effect on the magnitude of various elastic constant. Adjacent grain normally has different crystallographic orientation and a common grain boundary. The grain boundary acts as barrier to strain motion. Huge amount of lattice strain produced in nanomaterial prepared by the high energy mechanical milling¹⁸ should be taken into consideration. It is reported that average grain diameter decreases and strain increases with milling duration⁶. So with increasing milling time, due to the reduction in grain size, increase in values of elastic moduli is observed. Simultaneously, prolong milling induced strain naturally weakens the strength of elastic constant, which reveals the decrease in elastic constant for 24h milled sample for $x=0.6$ composition. The Debye temperature is the temperature at which maximum lattice vibrations take place. The observed increase in T_D with content (x) and milling time suggests that lattice vibrations are hindered due to the increase in strength of inter atomic bonding with replacement of Fe^{+3} by Al^{+3} and Cr^{+3} in $\text{CuAl}_x\text{Cr}_x\text{Fe}_{2-2x}\text{O}_4$ system.

Table 4. Molecular weight (M_1 , M_2), force constants (k_t , k_o) of A & B- sites respectively and average force constant (k), Bulk modulus (B), Young's modulus (E), rigidity modulus (G) and Poisson's ratio (V), Longitudinal elastic wave velocity (V_l), Transverse elastic wave velocity (V_s), Mean elastic wave velocity (V_m) and Debye temperature (T_D) for $CuAl_xCr_xFe_{2-2x}O_4$ ferrite system.

Elastic Parameter	x = 0.2			x = 0.6		
	Unmilled	Milled		Unmilled	Milled	
		12hrs	24hrs		12hrs	24hrs
M_1 (kg) $\times 10^{-3}$	50.846	54.503	62.780	58.160	60.47	51.616
M_2 (kg) $\times 10^{-3}$	117.86	114.202	105.925	97.456	95.146	104
k_t (N/m) $\times 10^2$	1.3043	1.4403	1.690	1.6173	1.6544	1.4434
k_o (N/m) $\times 10^2$	1.3866	1.3746	1.2642	1.2891	1.3368	1.4139
k (N/m) $\times 10^2$	1.3454	1.4074	1.4771	1.4532	1.4956	1.4287
B (GPa)	161.36	168.65	176.99	175.50	181.14	172.30
E (GPa)	145.22	151.79	159.27	157.95	163.03	155.09
G (GPa)	53.79	56.22	58.99	58.499	60.38	57.44
V	0.35	0.35	0.35	0.35	0.35	0.35
V_l (m/s)	5500.65	5630.77	5768.62	5844.01	5911.73	5802.35
V_s (m/s)	3175.80	3250.93	3330.51	3374.04	3413.14	3349.99
V_m (m/s)	4338.23	4440.85	4696.03	4609.02	4662.44	3716.23
T_D (K)	592.88	606.39	643.31	634.26	643.46	618.28

Conclusion

The study of the effect of mechanical milling on the structural properties, cation distribution and Infrared study of diamagnetic Al^{3+} and magnetic Cr^{3+} co-substituted Cu-ferrite, i.e. the nanostructured system with generic formula $CuAl_xCr_xFe_{2-2x}O_4$ is summarized as under.

The mechanical milling has much effect on structural and microstructural parameters. It is found that the milled samples of the system $CuAl_xCr_xFe_{2-2x}O_4$ exhibit Jahn-Teller structural deformation owing to the presence of Cu^{2+} and Cr^{3+} ions at octahedral sites of the spinel lattice. The study of unmilled and milled samples of the spinel system $CuAl_xCr_xFe_{2-2x}O_4$ reveals that the system exhibits tetragonal distortion and the distribution of the cations among the interstitial site is sensitive to the duration of milling of the samples. The observed change in IR absorption band position with milling time duration is mainly governed by reduction in grain size. The variation in elastic parameters is mainly governed by variation of lattice constant value and milling induced strain.

References:

1. Gleiter H., Nanocrystalline materials, Prog. Mater. Sci., 1989, 33, 223.
2. Jacob K. T., Alcock C. B., Metall.Trans, 1975, B6, 215.
3. Modi K. B., Shah S.J., Infrared spectral evolution, elastic, optical and thermodynamic properties study on mechanically milled $Ni_{0.5}Zn_{0.5}Fe_2O_4$ spinel ferrite, J. of Molecular structure, 2013, 1049, 250-262.
4. Chhantbar M. C., Ph. D. thesis, Saurashtra uni.2009.
5. Culity B.D., Elements of X-ray diffraction, 2nd ed., Addison-Wes-lye, NY 1978.
6. Vasoya N. H., Modi K. B., Synthesis of nanostructured material by mechanical milling and study on structural property modifications in $Ni_{0.5}Zn_{0.5}Fe_2O_4$, Ceramic International, 2010, 36, 947-954.
7. Smith J. and Wijn H. P. J., Ferrites, Philips, Eindhoven. 1959.
8. Burger M.J., Crystal structure Analysis, Wiley, NY, 1960.
9. Ohinishi H., Teranishi T., Crystal distortion in copper ferrite-chromite series, J. Phys. Soc. Jpn., 1961, 16, 35-43.
10. Miller A., Distribution of cations in spinels, J. Appl. Phys., 1959, 30, 24S-25S.

11. Johnson W.L., Thermodynamic and kinetic aspects of the crystal to glass transformation in metallic materials, Prog.Mater.Sci, 1986, 30, 81.
12. Globus A., Pascard H., Cagan V., Distance between magnetic ions and fundamental properties in ferrites, J. Phys. Suppl.,1977,438 (C-1) 163-168.
13. Siokafus K. E., Wills J. M., Grimes N. W., Structure of spinel, J. Am. Ceram. Soc., 1999, 82 (12), 3279-3292.
14. Henderson CMB., Charnock J.M. and Plant D.A., Cation occupancies in Mg, Co, Ni, Zn, Al ferrite spinels, J. Phys. Condens.Matter., 2007, 19, 076214.
15. Bellad S.S., Pujar R.B., Chougule B.K., Ind.J.PureAppl.phys, 1998, 36, 598.
16. Waldron R. D., Infrared spectra of ferrites, Phys. Rev., 1955, 99 (6) 1727.
17. Raj B., Rajendram V., Science and technology of ultrasonics, Narosa Pub. House, New Delhi, 2004,250
18. Bid S., Pradhan S.K., Characterization of crystalline structure of ball-milled nano-Ni-Zn-ferrite by Rietveld method, Mater. Chem. Phys., 2004, 84 (2-3) 291.
